

Effect of rotational speed on the hydraulic performance for flow conduits of shaft extension tubular pumping system

H Gao¹, F Yang^{1,*}, S J Chen¹ and Ch Liu^{1,2}

¹School of Hydraulic, Energy and Power Engineering, Yangzhou University, Yangzhou, Jiangsu, China

²Hydrodynamic Engineering Laboratory of Jiangsu Province, Yangzhou, Jiangsu, China

E-mail: fanyang@yzu.edu.cn

Abstract. In order to investigate the effect of rotational speed on hydraulic performance of inlet and outlet conduits for S-shaped shaft extension tubular pumping system, the three dimensional steady turbulent flow in pumping system was simulated using computational fluid dynamics technology. The experiment results are compared with the CFD results. The hydraulic performance parameters of inlet and outlet conduits were analyzed quantitatively considering the hydraulic interaction of conduits and impeller. The change trend of relationship curves between hydraulic loss ratio value and flow rate coefficient is same in different rotational speed. With the increase of flow rate coefficient, the hydraulic loss ratio value increases gradually, the hydraulic efficiency increases firstly then decreases gradually, and the average velocity circulation of outlet section increases firstly then decreases gradually in the same rotational speed. With the increase of rotational speed, the average velocity circulation increases gradually in the same flow rate coefficient. With the increase of flow rate coefficient, the relative swirl angle decreases firstly then increases in different rotational speed. With the increase of rotational speed, the static pressure ratio of outlet conduit increases gradually, and the distribution of drift angle in inlet section of outlet conduit is same. There is no linear functional relationship between the square of hydraulic loss and flow rate for outlet conduit.

1. Introduction

The flow conduits is an important part of the low-lift pump system, which has a significant effect on the hydraulic performance of the low-lift pump system [1-2]. The hydraulic performance of the flow conduits has been paid much attention by the scholars. The researchers have carried out some research work on the hydraulic characteristics of the low-lift pump system in order to improve the hydraulic performance of the low-lift pump system, and the research focuses on the three-dimensional optimization [3-6] and the flow field analysis [7-11] of the inlet and outlet conduits, the mechanism of the interaction between the pump and the flow in different working conditions [12-16]. Based on the analysis of the previous literature, the energy performance of the low-lift pump system is greatly affected by the hydraulic performance of the flow conduit. When the pumping station required flow rate, upstream and downstream water levels changes or serious cavitation appear and so on, the pump station often used variable speed adjustment mode, and the hydraulic performance parameter of the inlet and outlet flow conduits of the low-lift pump system is not clear when the rotating speed is



changed. In order to clarify the problem, the paper takes the S-shaped shaft extension tubular pumping system as the research object, the influence of speed on the hydraulic parameters of the flow conduit of the tubular pump is studied by using the three-dimensional numerical method.

2. Research object and simulation method

2.1. Research object

The S-shaped shaft extension tubular pumping system is equipped with an axial pump hydraulic model with a rotational speed of 1350, the nominal diameter of the runner is 0.30m, the tip clearance is 0.15mm, the hub ratio is 0.40, and the blade laying angle is 0° . The number of runner blades is 3, the number of leaf blades is 7, and the rated speed is 1450 r/min. The calculation area includes water inlet section, inlet conduit, runner, guide vane, outlet conduit and effluent section. The three-dimensional model of S-shaped shaft extension tubular pumping system is shown in figure 1.

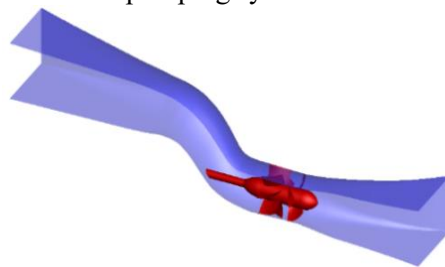


Figure 1. Shaft extension tubular pumping system

2.2. Simulation method

The runner and guide vane of the S-shaped shaft extension tubular pumping system are structured by the H/J/L-Grid and H-Grid topologies in the TurboGrid software. The inlet and outlet conduits use ICEM CFD Software carry out structured meshing. The grid quality has a great influence on the numerical calculation of the pumping system, and it needs to meet the requirement of no negative volume, grid orthogonality and aspect ratio in the calculation area. The grid orthogonality is ensured by the angle between any two faces of the element, and the lowest angle is between 15° and 165° . According to the Ref.[3,17-20] on the pumping system flow field calculation required for the number of grid, the number of grid required for the numerical calculation of the S-shaped shaft extension tubular pumping system is designed grid-independent analysis, the results shown in figure 2, when the pump system head coefficient and efficiency with the increase in the number of grids are less than 1% correlation, that the number of grid to meet the calculation requirements, the results are stable, The final determination of the S-shaped shaft extension tubular pumping system grid cell total of 1516416, the total number of grid nodes is 1628407.

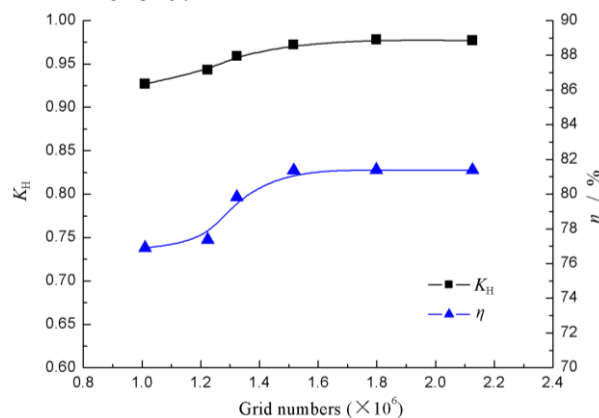


Figure 2. Verification of grid independence to prediction of performances

The RNG $k-\varepsilon$ turbulence model is used to calculate the turbulence field of the S-shaped shaft extension tubular pumping system. The near-wall region is treated with Scalable wall functions, and the convergence precision is set to 1.0×10^{-5} . The numerical calculator uses CFX-Solver Manager. The energy performance of five S-shaped shaft extension tubular pumping system at different speeds was calculated in this study, and the five rotational speeds are rated speed of 1.0 times (1450 r/min), 0.9 times (1305 r/min), 0.8 times (1160 r/min), 0.7 times (1015 r/min) and 0.6 times (870 r/min).

3. Performance prediction and verification

3.1. Experimental design

In order to further verify the accuracy of the numerical simulation results, the test is carried out on the high precision hydraulic machinery test-bed of Jiangsu Provincial Key Laboratory of Hydraulic Engineering. The comprehensive uncertainty of the high precision hydraulic machinery test-bed is $\pm 0.39\%$, which meet the accuracy requirements according of SL140-2006 *pump model and system model acceptance test procedures*, and through the national metrological review in 2015. The main technical parameters of the test-bed are: the flow test range is $0.1 \sim 0.5 \text{ m}^3/\text{s}$, the head test range is $-6.0 \sim 21.0 \text{ m}$, the torque test range is $0 \sim 500 \text{ N}\cdot\text{m}$, the speed test range is $0 \sim 2000 \text{ r/min}$. According to the energy test requirements of Section 6.1 of the SL140-2006 *pump model and system model acceptance test procedures*, before the energy test, ensure that the pump operating conditions in the absence of cavitation conditions for more than 30 minutes, excluding the free gas, bubbles and trapped gas in the system, collecting more than 15 different flow points.

Machining and numerical simulation of the same size of the physical model system, the model system shown in figure 3, the test rated speed is 1450 r/min, the blade laying angle is 0° .



Figure 3. Physical model of pumping system

3.2. Simulation and test verification

In order to greatly compare the results of numerical analysis and model test, the flow coefficient K_Q and the head coefficient K_H are used for comparative analysis. The results of numerical calculation and physical model test are shown in figure 4. The flow coefficient K_Q and the head coefficient K_H are calculated as:

$$K_Q = \frac{Q}{nD^3}; \quad K_H = \frac{gH}{n^2D^2} \quad (1)$$

Where: Q is the flow of the pump; H is the head of the pump; n is the speed; D is the nominal diameter of the runner, and g is the acceleration of gravity.

The predicted $K_Q \sim K_H$ curve of the S-shaped shaft extension tubular pumping system is consistent with the curve obtained by the physical model test. The predicted $K_Q \sim \eta$ curve of the S-shaped shaft extension tubular pumping system is in good agreement with the obtained curve, indicating the validity and reliability of the numerical results.

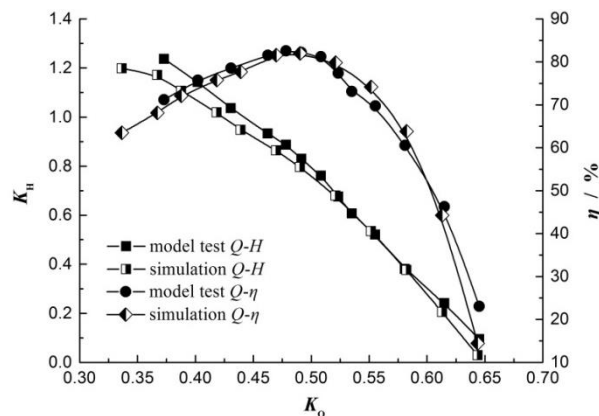


Figure 4. Comparison of the performance curves

4. Analysis of Influence of Speed on hydraulic performance of the flow conduit

4.1. Analysis of hydraulic performance of inlet conduit

In order to analyze the influence of speed on the hydraulic loss of the conduit, the hydraulic loss ratio β_j is introduced, which is the ratio of the hydraulic loss of the flow conduit to the head of the pump, and the formula is

$$\beta_j = \frac{\Delta h}{H} \times 100\% \quad (2)$$

Where: Δh is the hydraulic loss of the conduit; H is the pump head.

The influence of the speed on the hydraulic loss ratio β of the inlet runner is shown in Figure 5. The change trend of the hydraulic loss ratio of the inlet conduit and the flow coefficient is basically the same in different rotational speeds. In the same rotational speed, the hydraulic loss ratio of the inlet conduit increases with the increase of the flow coefficient. When the flow coefficient K_Q is in the range of 0.40 ~ 0.65, the hydraulic loss ratio of the inlet conduit decreases with the increase of the speed. When the flow coefficient K_Q is less than 0.40, the rotational speed has little effect on the hydraulic loss ratio of the inlet conduit. The rotation of the impeller causes the prerotation of the water to increase the water flow energy. The higher the rotational speed is, the more the water flow energy increases. Therefore, the hydraulic loss of the inlet conduit decreases.

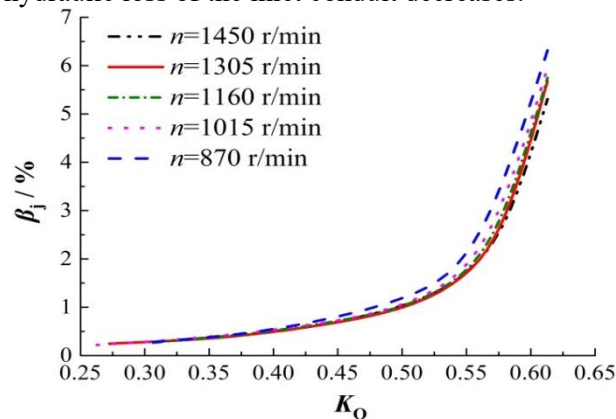


Figure 5. Ratio value of inlet conduit hydraulic loss

In order to further analyze the energy conversion efficiency of the inlet conduit, the homogenization efficiency of the flow conduit in Ref.[11] is calculated. The relationship between the hydraulic efficiency and the flow coefficient of the inlet conduit at different rotational speeds is shown

in Figure 6.

$$\eta_{av} = \frac{\sum_{i=1}^m \eta_i}{m}, \quad \eta_i = \frac{E_{out}}{E_{in}} \times 100\% \quad (3)$$

Where: η_{av} is the homogenization efficiency of the conduit; m is the total number of calculated operating conditions; E_{out} is the total energy of the outlet section of the conduit; E_{in} is the total energy of the inlet section of the conduit; η_i is the hydraulic efficiency of the inlet conduit for each condition; Let i denote different calculation conditions, $i=1, 2, \dots, m$.

At the same speed, the hydraulic efficiency of the inlet conduit decreases with the increase of the flow coefficient, but the decrease is very small. When the flow coefficient K_Q is in the range of (0.25 ~ 0.64), the range of the hydraulic efficiency of the inlet conduit is 0.264%, indicating that the change of the rotational speed has little effect on the hydraulic efficiency of the inlet conduit. The homogenization efficiency of the inlet conduit increases with the decrease of the rotational speed, and the homogenization efficiency of the inlet conduit is 99.88% when the speed is $n=870$ r/min, and the homogenization efficiency of the inlet conduit is higher increased about 0.29% than the rotational speed $n=1450$ r/min.

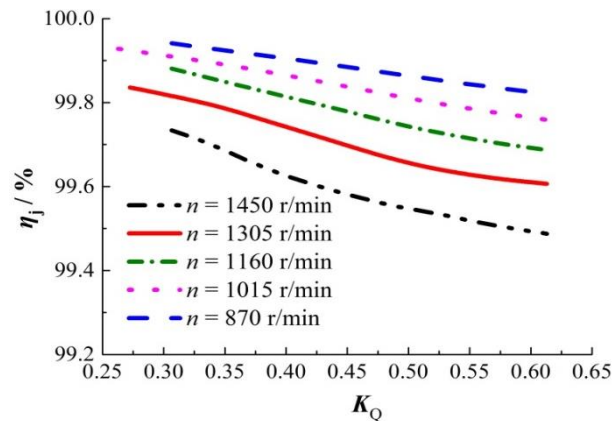


Figure 6. Hydraulic efficiency of inlet conduit

At different speeds, the relationship between the average circulation and the flow coefficient of the inlet conduit outlet section is shown in figure 7. At the same speed, the circulation of the inlet conduit decreases first and then increases with the increase of the flow coefficient. The difference of the average circulation is only $0.084\text{m}^2/\text{s}$ in the calculated operating range, and the difference is small. And the average circulation of the outlet section of the inlet conduit increases with the increase of the rotational speed in the same flow rate coefficient. The rotation of the impeller has a certain influence on the tangential velocity of the outlet section of the inlet conduit. When the same flow coefficient is calculated, the variation of the rotational speed is only $0.087\text{m}^2/\text{s}$, and the change of the rotational speed in the stable operation condition has little effect on the hydraulic performance of the inlet conduit, which is the same as that obtained in the Ref.[15].

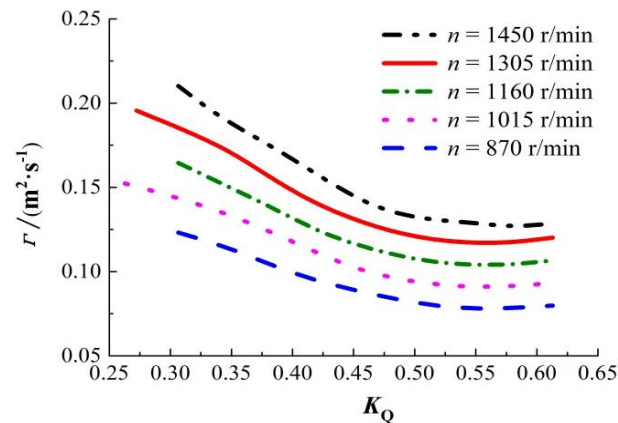


Figure 7. Average velocity circulation of outlet section in inlet conduit

For the quantitative analysis of the speed of the inlet conduit outlet velocity field, selecting the axial velocity of the inlet conduit outlet surface x direction (xyz coordinate direction is defined as shown in figure 1, z axis is the pump axis direction, x axis is the horizontal direction, y axis is the vertical direction) on the horizontal center line as the study object, and the definition of dimensionless distance l^* is

$$l^* = \frac{l_i}{l_b} \quad (4)$$

Where: l_i is the distance from the measuring point to the midpoint of the survey line; l_b is 0.5 times the total length of the line; i is the number of the measuring point.

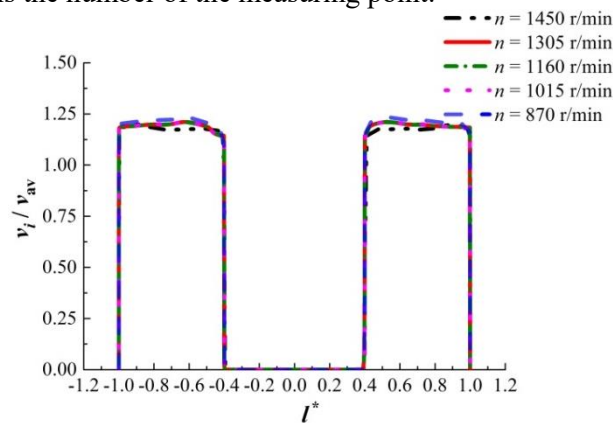


Figure 8. Relative axial velocity distribution of outlet section in inlet conduit

The axial relative velocity distribution of the x -axis direction of the outlet section in inlet conduit at the same flow coefficient $K_Q=0.50$ is shown in figure 8. The axial velocity in figure 8 is the ratio of the axial velocity to the average velocity v_i/v_{av} . The distribution of axial relative velocity on the horizontal center line of the outlet section in inlet conduit at different rotational speeds is basically the same, the velocity distribution is uniform, non-backflow and other bad flow appears. It is shown that the change of the rotational speed has little effect on the flow field of the outlet section in inlet conduit.

4.2. Analysis of hydraulic performance of the outlet conduit

The relationship between the relative swirl angle and the flow coefficient is shown in figure 9 at different rotational speeds, and the relative swirl angle of inlet section in outlet conduit is defined as

$$\alpha = \frac{\theta_i}{\theta_{\min}}, \quad \text{where: } \theta = \arctan \frac{v_t}{v_z} \quad (5)$$

Where: θ_{\min} is the minimum value of the inflow swirl angle in the calculation condition; v_t is the average tangential velocity; v_z is the average axial velocity.

The relative swirl angle decreases first and then increases with the increase of the flow coefficient at different speeds, the relationship between the relative value of the inflow swirl angle and the flow coefficient is an upward curve, and when the flow coefficient K_Q is in the range of 0.48 ~ 0.52, there is a minimum value of the relative inflow swirl angle, indicating that there is a minimum inflow swirl angle in the inlet section of the outlet conduit when the impeller speed is constant, mainly because the design of the guide vane is based on a single working condition. The inflow swirl angle in the inlet section of the outlet conduit is controlled by factors such as the residual circulation of the outlet of the guide vane and the inlet boundary condition of the outlet conduit. The flow field of the outlet conduit is complicated resulting in the relative value of the inflow swirl angle is not related to the speed at the same flow coefficient.

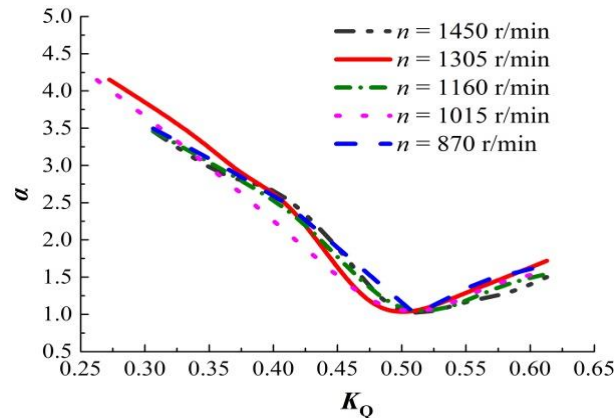


Figure 9. Relative swirl angle of inlet section in outlet conduit

The static pressure ratio of the outlet conduit at different rotational speeds is analyzed by static pressure ratio δ . And the static pressure ratio is calculated as

$$\delta = \frac{P_{out}}{P_{in}} \quad (6)$$

Where: p_{in} is the static pressure of the inlet surface of the conduit; p_{out} is the static pressure of the outlet surface of the conduit.

At different speeds, the static pressure ratio of the outlet conduit is shown in figure 10. When the flow coefficient K_Q is greater than 0.52, the increase of the static pressure ratio of the outlet conduit is larger; When the flow coefficient is less than 0.52, the static pressure ratio of the outlet conduit is relatively small. In the calculation range, the range of the static pressure ratio of the outlet conduit is 0.107. At the same flow coefficient, the static pressure ratio of outlet conduit increases slightly with the increase of the rotational speed, and the static pressure ratio of the outlet conduit increases with the increase of the rotational speed, when the rotational speed n increases from 870 r/min to 1450 r/min, the static pressure ratio is only increased by 0.069, the change of the rotational speed has little effect on the static pressure ratio of the outlet conduit.

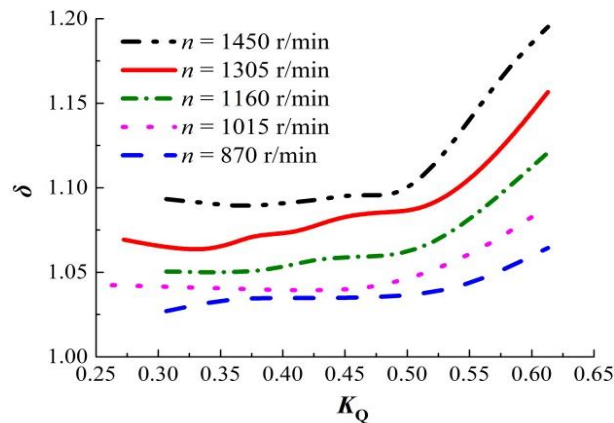


Figure 10. Static pressure ratio of outlet conduit

The same flow coefficient at different speeds $K_Q=0.50$, the distribution of drift angle in inlet section of outlet conduit is shown in figure 11, the drift angle is calculated as follows,

$$\gamma = \arctan \left| \frac{u_{ij}}{u_{aj}} \right| \quad (7)$$

Where: u_{aj} is the axial velocity of each unit in inlet section of outlet conduit; u_{ij} is the lateral velocity of each unit in inlet section of outlet conduit.

At the same flow coefficient, the distribution of drift angle in inlet section of outlet conduit is basically the same, and there are several small areas with large drift angle near the outlet of the rear guide cap. But the area of each region is not the same, the drift angle of the each water particle of the inlet surface is not symmetrical and the water flow does not enter the outlet conduit according to a fixed drift angle, the distribution of drift angle γ in the area of $6^\circ \sim 10^\circ$ is larger, and the distribution of the drift angle in inlet section of outlet conduit is affected by the residual circulation of the outlet of the guide vane, the internal flow field of the outlet conduit is easily calculated by the same drift angle boundary condition given by the inlet, and it is quite different from the actual situation.

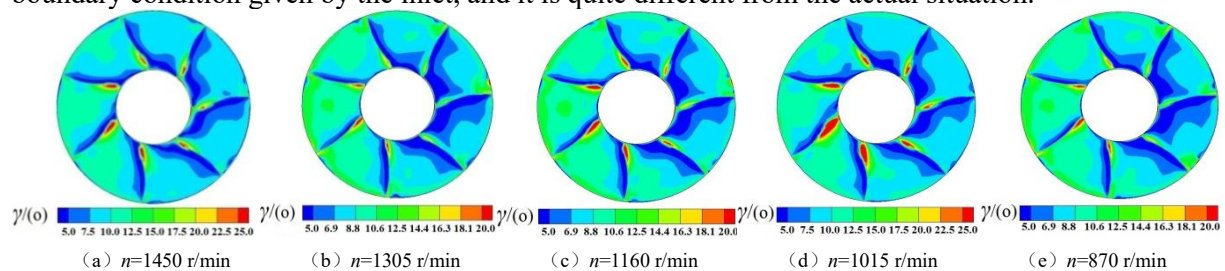


Figure 11. Distribution contours of drift angle in inlet section of outlet conduit

The relationship between the hydraulic loss ratio and the flow coefficient is shown in figure 12 at different rotational speeds. When the flow coefficient K_Q is less than 0.50, the difference between the hydraulic loss ratio and the flow coefficient of the outlet conduit at different rotational speeds is obvious, and the relationship between the hydraulic loss ratio of the outlet conduit and the change of the speed is not a certain; when the flow coefficient K_Q is greater than 0.50, The hydraulic loss ratio of the outlet conduit is similar to that of the flow coefficient at different rotational speeds; when the flow coefficient K_Q is in the range of $0.50 \sim 0.60$, the hydraulic loss ratio of the outlet conduit decreases with the increase of the rotational speed at the same flow coefficient; and when the flow coefficient is greater than 0.58, the hydraulic loss ratio of the outlet conduit has more than 30%. During the operation of different working conditions, the dominant factors of the hydraulic loss of the outlet

conduit are alternated by the hydraulic loss caused by the horizontal flow velocity and axial flow velocity. The hydraulic loss of the outlet conduit is dominated by the axial flow velocity when the flow is large, and dominated by the horizontal flow velocity when the flow is small, at this time, the residual circulation of the outlet of the guide vane is larger. Compared with the change of the hydraulic loss ratio of the inlet conduit, the hydraulic loss of the outlet conduit is more complicated with the variation of the flow coefficient, it is shown that the hydraulic loss of the outlet conduit does not satisfy the linear functional relationship with the second power of the flow velocity.

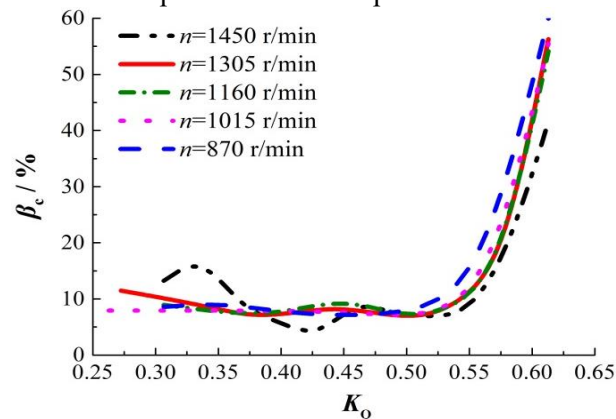


Figure 12. Ratio value of outlet conduit hydraulic loss

5. Conclusion

Based on the computational fluid dynamics ANSYS CFX software, the numerical simulation of the full conduit of the S-shaped shaft extension tubular pumping system is carried out. The predicted curve of the S-shaped shaft extension tubular pumping system $K_Q \sim K_H$ is consistent with the curve of the physical model test, the $K_Q \sim \eta$ curve is in good agreement with the experimental curve, which shows the validity and reliability of the numerical results.

The change trend of the hydraulic loss ratio of the inlet conduit and the flow coefficient is basically the same when the speed is different. At the same speed, with the increase of the flow coefficient, the hydraulic loss ratio of the inlet conduit also increases, and the hydraulic efficiency of the inlet conduit decreases gradually. At the same speed, the circulation of the outlet section of the inlet conduit decreases first and then increases with the increase of the flow coefficient. At the same flow coefficient, the average circulation of the outlet section of the inlet conduit increases with the increase of the rotational speed.

The relative swirl angle of the outlet conduit decreases first and then increases with the increase of the flow coefficient at different speeds, and there is a minimum value of the relative inflow swirl angle. At the same flow coefficient, the static pressure ratio of the outlet conduit increases slightly with the increase of the rotational speed, and the static pressure ratio of the outlet conduit increases with the increase of the rotational speed. At the same flow coefficient, the distribution of drift angle in inlet section of outlet conduit is basically the same, and the drift angle of the each water particle of the inlet surface is not symmetrical.

Acknowledgements

This research work was supported by the National Natural Science Foundation of China (Grant no. 51609210), Natural Science Foundation of Jiangsu Province (Grant no. BK20150457), China Postdoctoral Science Foundation (Grant no. 2016M591932), the open research subject of Key Laboratory of Fluid and Power Machinery, Ministry of Education (szjj2016-078) and the Priority Academic Program Development of Jiangsu High Education Institutions (PAPD).

References

- [1] Liu Chao. Researches and developments of axial-flow pump system[J]. Transactions of the Chinese Society for Agricultural Machinery, 2015, 46(6): 49-59. (in Chinese)
- [2] Lu Lin Guang. Optimized hydraulic design of high performance large - scale low -lift pump [M]. Bei Jing: China Water Conservancy and Hydropower Press, 2013. (in Chinese)
- [3] Wang Zhengwei, Peng Guangjie, Zhou Lingjiu, et al. Hydraulic performance of a large slanted axial-flow pump[J]. Engineering Computations, 2010, 27(2): 243-256.
- [4] Shi Weidong, Zhang Desheng, Guan Xingfan, et al. Optimization and experimental investigation on post bulb type tubular pump device model[J]. Journal of Hydraulic Engineering, 2010, 41(10): 1248-1253. (in Chinese)
- [5] Huang Liangyong, Wu Zhong, Zhang Xiao, et al. Hydrodynamic optimization of large pump installation with two-way channel and experiment[J]. Journal of Drainage and Irrigation Machinery Engineering, 2016, 34(7): 602-607. (in Chinese)
- [6] Shi Lijian, Tang Fangping, Liu Xueqin, et al. Optimization design and experiment of large cube-type pump device[J]. Transactions of the Chinese Society for Agricultural Machinery, 2017, 48(1): 96-103. (in Chinese)
- [7] Liu Houlin, Zhou Xiaohua, Wang Kai, et al. Analyzing flow patterns and hydraulic performance of volute intake sump for pump station[J]. Journal of Huazhong University of Science and Technology: Natural Science Edition, 2013, 41(11): 12-16. (in Chinese)
- [8] Chang Jingcai, Wang Zhiqiang, LI Xingping, et al. Study on hydraulic characteristics of new bell suction duct in large-scale pumping stations[J]. Journal of Hydroelectric Engineering, 2011, 30(1): 165-169, 179. (in Chinese)
- [9] Yan Hao, Liu Meiqing, Zhao Wensheng, et al. Influence of velocity circulation on hydraulic performance of large axial-flow pumps station[J]. Journal of Central South University (Science and Technology), 2016, 47(6): 2125-2132. (in Chinese)
- [10] Chen Songshan, Yan Hongqin, Zhou Zhengfu, et al. Three-dimensional turbulent numerical simulation and model test of front-shaft tubular inlet conduit of pumping system[J]. Transactions of the CSAE, 2014, 30(2): 63-71. (in Chinese)
- [11] Zhou Daqing, Liu Min, Chen Huixiang. Siphon outlet conduit on full passage cavitation characteristics of axial-flow pumping unit[J]. Journal of Huazhong University of Science and Technology (Nature Science Edition), 2017, 45(1): 128-132. (in Chinese)
- [12] Yang Minguan, Meng Yu, Li Zhong, et al. Design of axial-flow impeller guide cone and simulation on hydraulic performance of its passage[J]. Transactions of the CSAE, 2015, 31(11): 81-88. (in Chinese)
- [13] Yang Fan, Xie Chuanliu, Liu Chao, et al. Influence of axial-flow pumping system operating conditions on hydraulic performance of elbow inlet conduit[J]. Transactions of the Chinese Society for Agricultural Machinery, 2016, 47(2): 15-21. (in Chinese)
- [14] Lu Weigang, Dong Lei, WANG Zhaofei, et al. Cross influence of discharge and circulation on head loss of conduit of pump system with low head[J]. Applied Mathematics and Mechanics: English Edition, 2012, 33(12): 1533-1544.
- [15] Chen Wei, Lu Linguang, Wang Gang, et al. Influence of axial-flow pump operating condition on the pre-swirl at impeller chamber inlet[J]. Journal of Hydroelectric Engineering, 2012, 31(1): 213-219, 225. (in Chinese)
- [16] Yang Fan, Liu Chao, Tang Fangping, et al. Analysis of hydraulic performance of outlet passage based on simulation of steady flow in whole passage of axial-flow pumping system[J]. Transactions of the Chinese Society for Agricultural Machinery, 2014, 45(3): 83-89. (in Chinese)
- [17] Kim Jin-Hyuk, Ahn Hyung-Jin, Kim Kwang-Yong. High-efficiency design of a mixed-flow pump[J]. Science China Technology Science, 2010, 53(1): 24-27.

- [18] Wang Ling, Li Min, Wang Fujun, et al. Study on three-dimensional internal characteristics method of suter curves for double-suction centrifugal pump[J]. Journal of Hydraulic Engineering, 2017, 48(1): 113-122. (in Chinese)
- [19] Liu Jiantao, Liu Shuhong, Sun Yuekun, et al. Three-dimensional flow simulation of transient power interruption process of a prototype pump-turbine at pump mode[J]. Journal of Mechanical Science and Technology, 2013, 27(5): 1305-1312.
- [20] A. Lucius, G.Brenner. Unsteady CFD simulations of a pump in part load conditions using scale-adaptive simulation[J]. International Journal of Heat and Fluid Flow, 2010(31): 1113-1118.